

Short Communication

Foliated natural graphite as the anode material for rechargeable lithium-ion cells

Kenji Fukuda^a, Kazuhiko Kikuya^b, Kennichi Isono^b, Masaki Yoshio^{b,*}

^a Mitsui Mining Co., Ltd., 1–3 Hibikimachi, Wakamatsu-ku, Kitakyushu 808, Japan

^b Department of Applied Chemistry, Saga University, Saga 840, Japan

Received 18 November 1996; accepted 25 January 1997

Abstract

Natural graphite with a high capacity for lithium-ion cells is obtained by the chemical flaking of natural graphite along cleavage planes. Flaking of graphite (foliated graphite) is obtained via: (i) formation of expanded graphite from natural graphite by acid treatment, and (ii) mechanical and ultrasonic powdering of expanded graphite. This treatment is useful even for natural graphite, that contains a large ash content, which shows very poor capacity and large polarization. © 1997 Elsevier Science S.A.

Keywords: Graphite; Carbon; Lithium-ion cells; Battery materials

1. Introduction

During the past several years, many carbonaceous graphites, such as natural graphite, cokes and graphitized carbons, have been widely investigated as the alternative anodes for rechargeable lithium-ion cells. Among the many types of carbon anodes, natural graphite appears to be a most desirable candidate due to its high capacity, low cost and low electrode potential relative to lithium metal. In practical applications, however, a number of problems with graphite anode have still to be overcome in order to improve rate capability and cycleability. In particular, the performance of the graphite anode is influenced strongly by both the cycling rate and the electrode thickness [1]. This is mainly associated with morphological aspects of the compound (e.g. particle size, surface area and crystallinity). The present work reports the electrochemical performance of a foliated graphite as an anode for lithium-ion cells.

2. Experimental

Two kinds of natural graphite (NGr), namely, China graphite (ash 0.3%) (NGrCH) and Madagascar graphite (ash 9.2%) (NGrMD) were used as the starting material. Foliated graphite (FGr) was obtained via: (i) natural graphite, as received, was immersed in a H₂SO₄/HNO₃ (9:1 in

v/v ratio) mixed acid solution for 2 h and intercalation of sulfuric acid was carried out between the graphite layers; then, it was filtered off and washed with water; (ii) the resulting material was heated at 1000 °C under a nitrogen gas atmosphere to form expanded graphite (EGr) and was then ground into a powder, and (iii) ground EGr was dispersed into water and powdered further using an ultrasonic method. Thus, foliated graphite (FGr) was formed.

The charge and discharge characteristics of NGr, EGr and FGr were examined in coin-type cells. The cell comprised a graphite electrode and a lithium metal with a separator in between. The graphites (5 to 15 mg) were mixed with 5 wt.% ethylenepropylenedien polymer (EPDM) as a binder dissolved in *n*-hexane. The paste mixture was spread thinly on a stainless-steel mesh and pressed at 1 ton cm⁻². The electrodes were dried under vacuum at 200 °C for 2 h. The electrolyte was a 1 M LiPF₆-ethylene carbonate (EC)/dimethyl carbonate (DMC) (1:2 in volume). Galvanostatic charge and discharge were carried out between 1.5 and 0.001 V at, typically, 0.4 mA cm⁻².

3. Results and discussion

The crystallite parameters L_a , L_c and $d_{(002)}$ were calculated using the following equations from the X-ray diffraction patterns (XRD) of the test graphite materials:

* Corresponding author. Tel.: 81 952 28 8673; Fax: 81 952 28 8591.

Table 1
Some physical properties of graphites

Graphite type	Mean particle size (μm)	Mean particle thickness (μm)	Ash content (wt.%)	Specific surface area ($\text{m}^2 \text{g}^{-1}$)	d_{002} (nm)	$L_c(002)$ (nm)	$L_a(110)$ (nm)	n -value
NGr CH	1160	38	0.3	0.6	0.335	129	201	294
EGr CH	25	5	0.3	17.1	0.335	79	115	63
FGr CH	25	0.1	0.3	17.6	0.335	69	25	1.5
NGr MD	246	15	9.2	2.2	0.335	292	538	54
EGr MD	25	3	6.4	15.8	0.335	49	66	61
FGr MD	25	0.1	6.3	23.0	0.335	48	59	2

$$L_a(110) = \frac{0.89s}{[B_{110} \cos(\theta_{110})]} \quad (1)$$

$$L_c(002) = \frac{0.89s}{[B_{002} \cos(\theta_{002})]} \quad (2)$$

where s is the wavelength of Cu K α ($s = 0.15418 \text{ nm}$), B_{110} and B_{002} are the width at half-maximum of the (100) and (002) diffraction peaks, θ_{110} and θ_{002} are the corresponding Bragg diffraction angles.

From the results given in Table 1, it can be seen that the mean particle size and thickness decrease in the order: NGr > EGr = FGr. The values of d_{002} of the EGr and FGr compounds are essentially the same as those of the as-received graphites (NGrs). A marked decrease in the values

of $L_c(002)$ and $L_a(110)$ for FGrs was observed compared with those for the NGrs.

The morphological changes on going from NGr to EGr and FGr can be explained in terms of the degree of graphite foliation in the thickness direction. The mean number of crystallites in a thickness direction of graphite particles (n -value) may be defined as follows

$$n = \frac{\text{mean particle thickness}}{L_c(002)} \quad (3)$$

The n -value may also be defined as the thickness of the slab of graphite layers along the c -axis. NGrCH has a thickness of $38 \mu\text{m}$ and an $L_c(002)$ of 129 nm . Thus, thickness of the slab is around 300. The n -values for EGrCH and FGrCH are

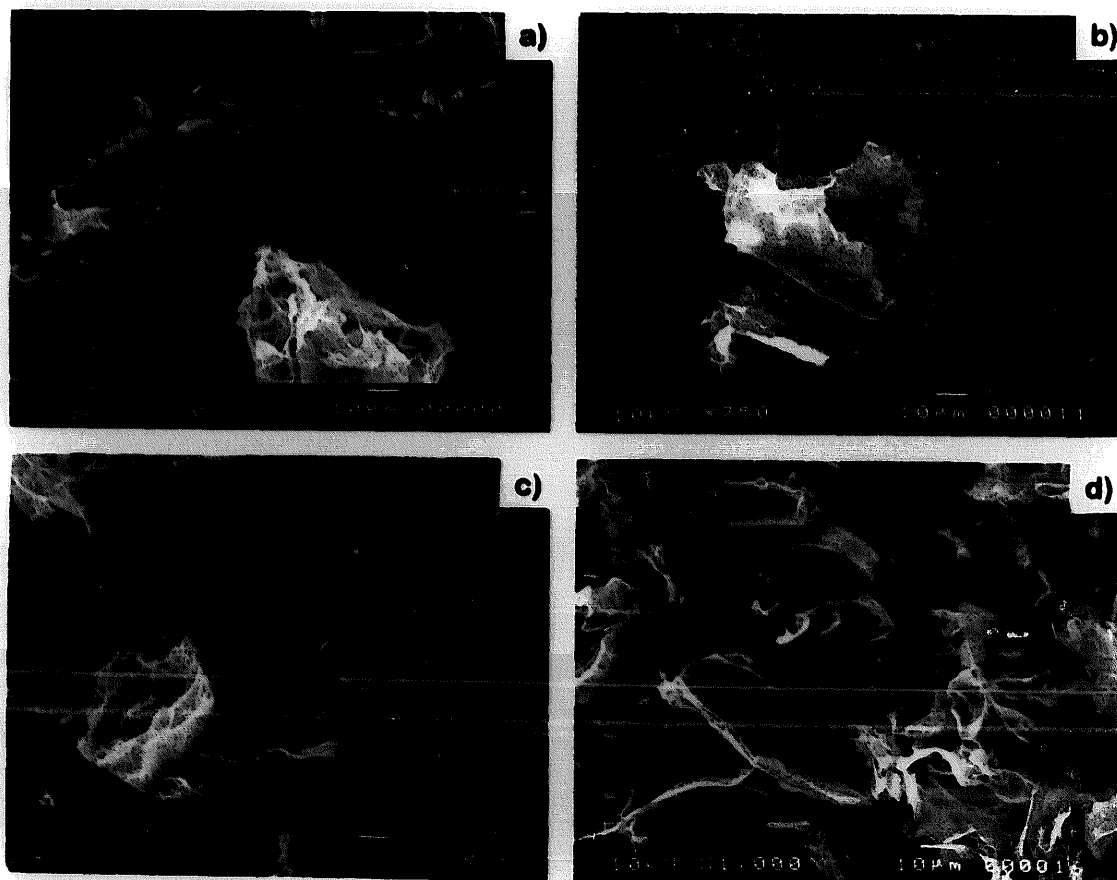


Fig. 1. SEM graphs of foliated graphite obtained from China graphites: (a) EGrCH (b) FGrCH, and Madagascar graphites: (c) EGrMD, (d) FGrMD graphite.

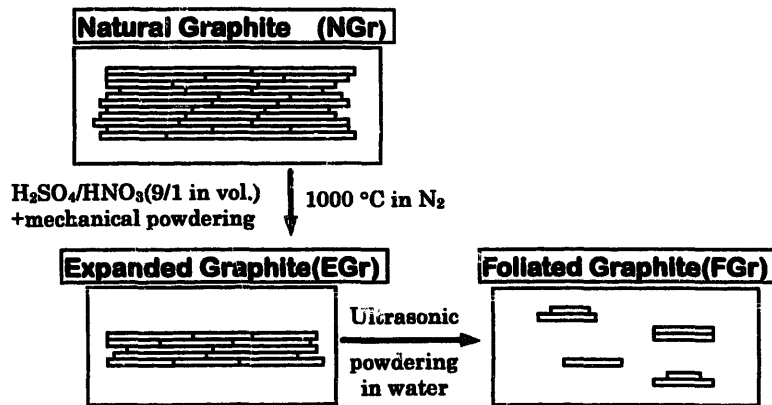


Fig. 2. Schematic of the morphological changes between NGr, EGr and FGr.

63 and 1.5, respectively. This indicates that the graphite layer along the c -axis is effectively divided by the formation of EGr following ultrasonic powdering. The n -values of all graphite samples decrease in the order: $\text{NGr} > \text{EGr} > \text{FGr}$. Finally, the n -values of the FGr are ~ 1 –2, which means that all the graphite layers are ideally separated. This is clearly seen in electron micrographs of EGr and FGr, which have very thin particle graphite, as shown in Fig. 1. A schematic of the morphological changes with respect to changes in the n -value is shown in Fig. 2. The $L_a(110)$ values also decrease in the order: $\text{NGr} > \text{EGr} > \text{FGr}$. Flaking of graphite perpendicularly to c -axis also takes place. The surface area of NGr is increased during the formation of EGr.

An examination was made of the effect of the above morphological changes on the performance of lithium-ion cells. Typical charge and discharge curves of NGr, EGr and FGr at a current of 0.4 mA cm^{-2} are shown in Figs. 3 and 4, respectively. NGrMD with a high ash content displays poor rechargeable capacity (90 mAh g^{-1}) and high polarization. The rechargeable capacities of EGrMD, FGrMD, NGrCH, EGrCH and FGrCH are 305, 313, 219, 349 and 370 mAh g^{-1} , respectively. Obviously, a marked improvement in cell performance was obtained with FGr by virtue of the foliation

of the natural graphites. The capacity of FGrCH is very close to the theoretical LiC_6 value, namely 372 mAh g^{-1} .

The relation between rechargeable specific capacity and crystallite parameters was also investigated. Franklin's p -value [2] represents the probability of the existence of random disorientation in a graphite layer, which is calculated according to

$$d_{002} = 3.440 - 0.086(1 - p^2) \quad (4)$$

The crystallinity of the graphite increases when the p -value is decreased from 1 to 0. The p -values of all the graphites investigated are found to be essentially zero, as shown in Table 2. This indicates that all the graphites are highly crystalline. The rechargeable capacities of China and Madagascar graphites obtained at current densities of 0.4 mA cm^{-2} are listed in Table 2. The data demonstrate that it is difficult to evaluate the electrochemical performance of graphite based on the Franklin's p -value.

Fujimoto et al. [3] have proposed the following relationship between the reversible specific capacity ($Q \text{ mAh g}^{-1}$) and the crystallite parameters of graphite

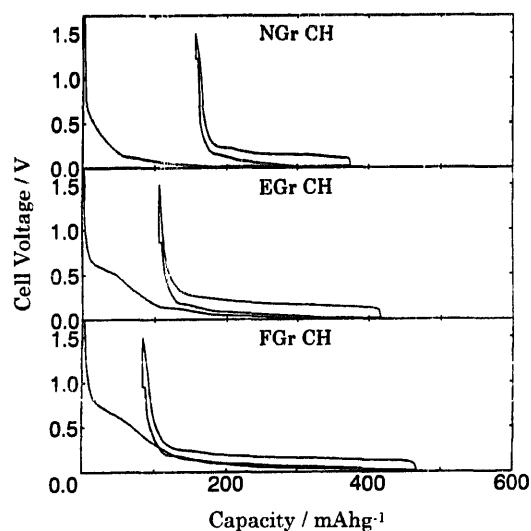


Fig. 3. Initial charge/discharge curves at a current density of 0.4 mA cm^{-2} for China graphites: NGrCH, EGrCH and FGrCH.

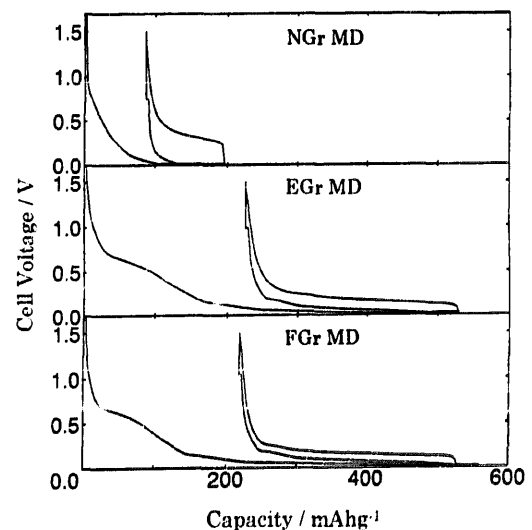


Fig. 4. Initial charge/discharge curves at a current density of 0.4 mA cm^{-2} for Madagascar graphites: NGrMD, EGrMD and FGrMD.

Table 2
Observed and estimated rechargeable capacity, Q , and some physical properties of graphites

Graphite	Franklin's p -value [2]	Q -value ^a [3]	Pr -value [4]	Q -value ^b [4]	Observed rechargeable capacity, Q (mAh g ⁻¹)
NGr CH	≈ 0	370	0.69	115	219
EGr CH	≈ 0	368	≈ 0.1	335	349
FGr CH	≈ 0	363	≈ 0.1	335	370
NGr MD	≈ 0	371	0.39	227	137
EGr MD	≈ 0	367	≈ 0.4	223	305
FGr MD	≈ 0	366	≈ 0.3	260	313

^a Refer Eq. (6).

^b Refer Eq. (7).

$$Q = \frac{372}{\left[1 + \frac{d_{002}}{L_c}\right] \left[1 + 2d_{c-c} \frac{(\sqrt{3}L_u + d_{c-c})}{(L_u^2 + d_{c-c}^2)}\right]} \quad (5)$$

where d_{c-c} is the distance between two neighboring carbon atoms in the same graphite plane (nearly equal to 0.142 nm). Since L_u is much larger than d_{c-c} in natural graphites, Q may be written as follows

$$Q = \frac{372}{\left[1 + \frac{d_{002}}{L_c}\right] \left[1 + \frac{2\sqrt{3}d_{c-c}}{L_u}\right]} \quad (6)$$

Given higher the values of L_u and L_c , the capacity of the graphite is larger. The capacity calculated from Eq. (6) would, however, be fundamentally the same (as shown in Table 2) because the natural graphite has much larger L_c and L_u values compared with d_{002} and d_{c-c} . It is concluded that this method would not reflect the difference in structure between graphites as investigated by Franklin's p -value.

We have found a much better relationship between the graphitic carbon and the corresponding rechargeable capacity. Zheng et al. [4] have proposed that Q can be represented as

$$Q = 372(1 - Pr) \quad (7)$$

where Pr represents the probability of random stacking. The values of Pr and calculated capacities for the present study are listed in Table 2. The probability of random stacking is decreased by the foliation of graphite while the battery performance is increased. Both FGr's, with low Pr values, deliver high rechargeable capacities, as expected from Eq. (7). This method would be useful to explain the rechargeable capacity of graphitic carbons, although the linear relationship between the capacity and $(1 - Pr)$ is not well defined.

Manev et al. [5] reported the effect of the splitting of natural graphite into layered slabs on the performance of

lithium-ion cells [5]. In their method, the ground natural graphite was dispersed in water in a high-speed mixer in the presence of surfactants and a high capacity graphite was obtained. According to the results presented here, finely foliated graphite delivers a high rechargeable capacity. The degree of foliation can be represented by the n -value, which is defined as thickness/ L_c . The value of 1 to 2 gives an ideal rechargeable capacity. Since the n -value depends on the thickness of the graphite particles, the mechanical and chemical powdering processes are very important. Formation of expanded graphite and subsequent ultrasonic powdering yields ideal flaking along the c -axis.

4. Conclusions

By applying chemical flaking that includes ultrasonic powdering of natural graphites, it is possible to obtain electrodes with specific rechargeable capacities that are very close to the theoretical value of 372 mAh g⁻¹ for LiC₆. The method presented here is suitable for natural graphite with a high content of ash and its performance is improved markedly to give a large capacity of over 320 mAh g⁻¹. This makes natural graphite a promising low cost anode material for rechargeable lithium-ion cells.

References

- [1] Z.X. Shu, R.S. McMillan and J.J. Murray, *J. Electrochem. Soc.*, 140 (1993) 992.
- [2] R.E. Franklin, *Acta Crystallogr.*, 4 (1951) 253.
- [3] H. Fujimoto, A. Mabuchi, K. Tokumitsu, T. Kasuh and N. Akuzawa, *Carbon*, 32 (1994) 193.
- [4] T. Zheng, J.N. Reimers and J.R. Dahn, *Phys. Rev. B*, 51 (1995) 734.
- [5] V. Manev, I. Naidenov, B. Puresheva, P. Zlatilova and G. Pistoia, *J. Power Sources*, 55 (1995) 211.